Clim Dyn
DOI 10.1007/s00382-008-0513-4

# Response of the Western European climate to a collapse of the thermohaline circulation

**A. Laurian · S. S. Drijfhout · W. Hazeleger · B. van den Hurk**

Received: 12 September 2008 / Accepted: 15 December 2008


**Abstract** Two ensemble simulations with the ECHAM5/MPI-OM climate model have been investigated for the atmospheric response to a thermohaline circulation (THC) collapse. The model forcing was specified from observations between 1950 and 2000 and it followed a rising greenhouse gases emission scenario from 2001 to 2100. In one ensemble, a THC collapse was induced by adding freshwater in the northern North Atlantic, from 2001 onwards. After about 20 years, an almost stationary response pattern develops, that is, after the THC collapse, global mean temperature rises equally fast in both ensembles with the hosing ensemble displaying a constant offset. The atmospheric response to the freshwater hosing features a strong zonal gradient in the anomalous 2-m air temperature over Western Europe, associated with a strong land–sea contrast. Since Western Europe climate features a strong marine impact due to the prevailing westerlies, the question arises how such a strong land–sea contrast can be maintained. We show that a strong secondary cloud response is set up with increased cloud cover over sea and decreased cloud cover over land. Also, the marine impact on Western European climate decreases, which results from a reduced transport of moist static energy from sea to land. As a result, the change in lapse rate over the cold sea surface temperature (SST) anomalies west of the continent is much larger than over land, dominated by changes in moisture content rather than temperature.

A. Laurian (✉) · S. S. Drijfhout · W. Hazeleger · B. van den Hurk
KNMI, Royal Netherlands Meteorological Institute, De Bilt, The Netherlands
e-mail: laurian@knmi.nl

**Keywords** Climate change · Thermohaline circulation · Western Europe · Ocean–atmosphere interactions · Land–sea contrast · Lapse rate

## 1 Introduction

The thermohaline circulation (THC) is a key component of the climate system. It transports large amounts of heat and salt poleward (Manabe and Stouffer 1999; Bryden et al. 2005). A change in the strength of the THC leads to large global and regional climate changes (Vellinga and Wood 2002). Observations in the North Atlantic Ocean indicate that the THC is about 18.7 ± 5.6 Sv (1 Sv = $10^6$ $m^3$ $s^{-1}$; Cunningham et al. 2007). In models, the THC has two stable equilibria which depend on the oceanic conditions (Manabe and Stouffer 1988). When the THC resides in the multiple equilibria regime, a freshwater pulse may lead to a collapse. Under global warming, a gradual weakening of the North Atlantic THC by 25(±25)% is expected for 2100 (Schmittner et al. 2005). Current climate models do not project a collapse of the THC in the twenty-first century, but the stability characteristics are not well known (Yin and Stouffer 2007). Sensitivity studies with climate models with a forced collapse provide scenarios on what would happen if the THC collapsed.

A collapse of the THC results in a reduced poleward oceanic heat transport and an increased poleward atmospheric heat transport (Cheng et al. 2007). In response to the collapse, SST decreases over the North Atlantic Ocean and increases in the South Atlantic Ocean, leading to a southward shift of the Intertropical Convergence Zone (Stouffer et al. 2006; Dong and Sutton 2002). These responses can lead to global changes such as the triggering of an El Niño event (Dong and Sutton 2002) or the

Published online: 29 January 2009

reduction of African monsoonal winds and rainfall over West Africa (Chang et al. 2008).

The issue of land–sea contrast has recently been investigated by Sutton et al. (2007) in response to a greenhouse gas forcing and by Joshi et al. 2008; hereafter, Joshi08) in response to a homogeneous temperature forcing. Both studies showed that in response to global temperature change, temperatures over land change more rapidly than over sea. However, over Western Europe, the response of climate to a collapse of the THC is largest over the cold SST anomalies to the west of the continent.

In this paper, we investigate this response in a climate change scenario using output from two-five-member ensemble simulations performed with the ECHAM5/MPI-OM climate model. We seek to understand why a collapse of the THC induces a strong land–sea contrast in the 2-m air temperature response over Western Europe where a strong marine impact due to prevailing westerlies is expected to lead to a weak contrast. We suggest physical mechanisms to account for the strong regional land-sea contrast in particular in the 2-m air temperature response with the anomaly over sea exceeding the anomaly over land.

## 2 Model and experiment

We use the ECHAM5/MPI-OM climate model developed at the Max-Plank Institute for Meteorology in Hamburg (Roeckner et al. 2003; Marsland et al. 2003). The atmospheric component has a horizontal resolution of T63 and has 31 levels in the vertical. The ocean model has a bipolar grid. Away from the poles (which are placed over Greenland and West Antarctica), the horizontal resolution is approximately 1.4° by 1.4°, but near the equator, the meridional resolution is refined to 0.5°. Near the poles, the resolution is highest: O(20–40 km). The ocean model has 40 levels in the vertical.

A 17-member ensemble of model simulations was performed over the period 1950–2100 as part of the ESSENCE project (Sterl et al. 2008). From 1950 to 2000, the simulations were forced by the concentrations of greenhouse gases (GHG) and tropospheric sulfate aerosols specified from observations. From 2001 to 2100, the simulations followed the SRES A1b scenario (Nakicenovic et al. 2000). Each simulation was initialized from a single long simulation, in which historical GHG concentrations have been used until 1950. For each ensemble member Gaussian noise of 0.1 K was added to the initial atmospheric temperature field. The initial ocean state was not perturbed.

Here, we investigate two-five-member ensemble simulations taken from the same 17-member ensemble having exactly the same initial conditions and the same initial forcing. In one ensemble, a freshwater anomaly of 1 Sv was uniformly applied over the northern North Atlantic Ocean between 50°N and 70°N from 2001 onwards, starting from five initial states of the other ensemble. This freshwater supply leads to a collapse of THC within 20 years. In the other ensemble the THC gradually weakens by 20% after 100 years due to global warming. The motivation for these simulations was the question how global warming would evolve when a THC collapse would occur during the warming episode. It appears that an almost stationary anomaly pattern develops that is the fingerprint of the THC on the atmosphere. In this paper we investigate this anomaly pattern with a focus on the 2-m air temperature response, and how this pattern is maintained, using monthly mean output from both ensembles. The ensemble mean of the perturbed simulations (called HOSING) is compared to the ensemble mean of the associated control simulations (called ENSMALL) over the period 2091–2100 in the Western Europe region, defined by 30°W–20°E, 30°N–60°N.

## 3 Regional temperature response over land and sea

The primary response to a THC collapse is ocean-driven, given the freshwater supply over the northern North Atlantic. Due to the additional freshwater, deep convection is reduced in the Atlantic and SSTs and sea-ice coverage changes in the subpolar North Atlantic. In a later stage, SSTs change over a larger area because of advection of anomalous SST, changing ocean currents and changing winds. Therefore, the primary air temperature change associated with a THC collapse must be different over the ocean than above land (Chang et al. 2008). In regions with a strong marine influence, however, one may expect that the prevailing westerly winds reduce or even level out such land-sea differences, and that the primary temperature response of the atmosphere is modulated by the dynamics. Indeed, the transport of moist static energy (called MSE, $\mathrm{MSE} = gz + c_pT + L_vq$ with $g$ the gravitational constant, $z$ the height, $c_p$ the heat capacity of air, $T$ the temperature, $L_v$ the latent heat and $q$ the specific humidity) by the mean winds is eastward (Fig. 1a). Moreover, there is a positive convergence of MSE, meaning that the MSE flux decreases eastward most notably between 36° and 52°N. The equilibrium 2-m air temperature response over Western Europe is shown in Fig. 1b. It features a stronger cooling above the ocean (about 5.5°C in annual mean) than above land (about 2.5°C in annual mean) suggesting that the role of dynamical processes in reducing the land–sea contrast is weak. It is noteworthy that in other regions (i.e. away from the cold SST anomaly located between 30°W and the Western

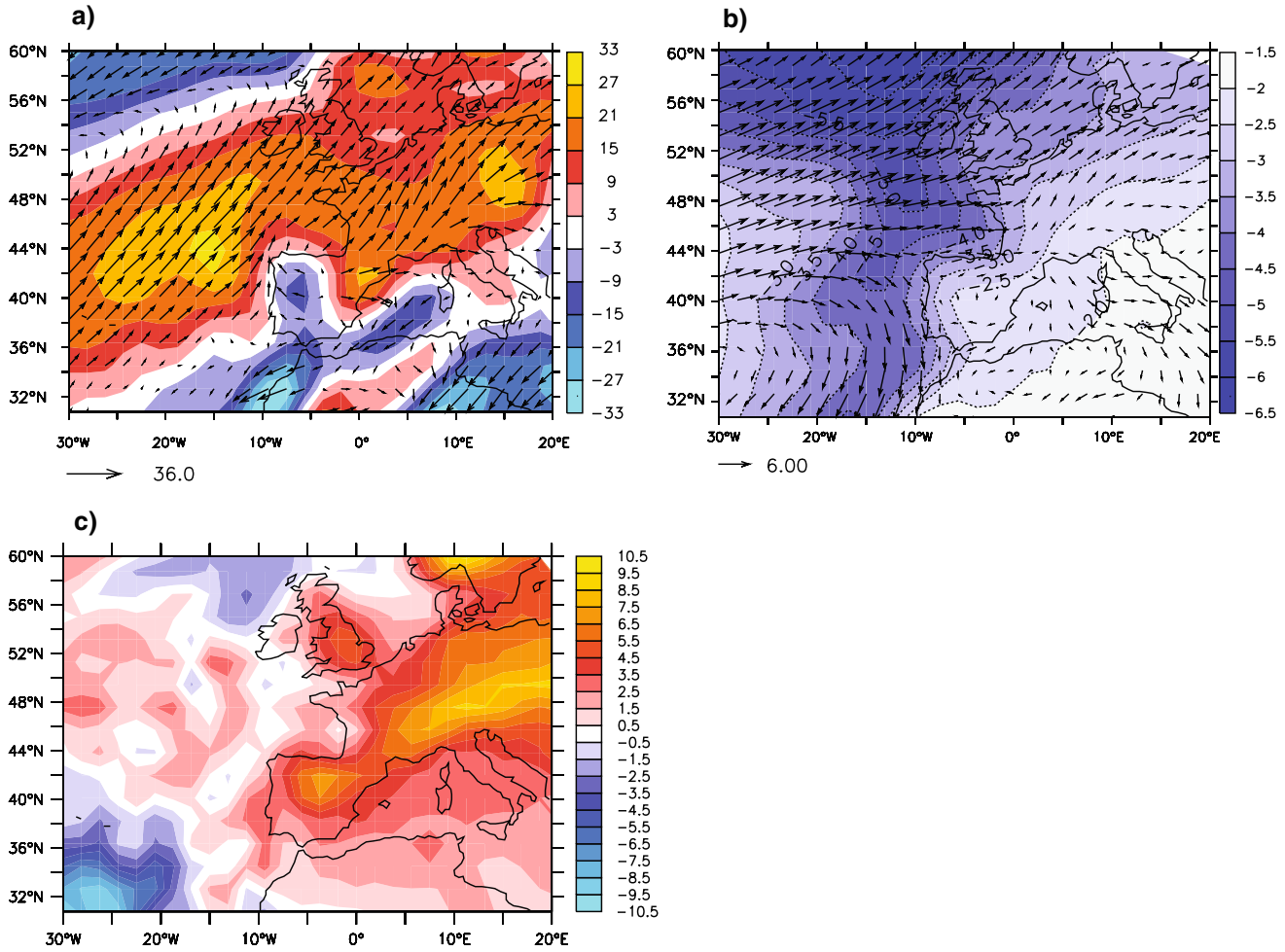


**Fig. 1** **a** Annual mean column-integrated convergence of zonal moist static energy transport ($m^3\ s^{-3}$) over the period 2091–2100 in ENSMALL. The annual mean column-integrated MSE flux is shown by the *arrows*. **b** Annual mean change in 2-m air temperature (°C) over the period 2091–2100 calculated as the difference between HOSING and ENSMALL. The annual mean 2-m winds in ENSMALL are shown by the *arrows* (in $m\ s^{-1}$). **c** Net top of the atmosphere heat flux anomalies (positive downward; in $W\ m^{-2}$)

European coastline) the land–sea contrast can be weaker or even reversed. The seasonal cycle in the cooling pattern of Fig. 1b is weak, even though the cooling penetrates more over land in winter than in summer due to stronger westerlies in winter (not shown). The annual mean pattern of the 2-m temperature change is in agreement with the AOGCM intercomparison performed by Stouffer et al. (2006) and with results from Vellinga and Wood (2002, 2006), Cheng et al. (2007), and Chang et al. (2008).

The question arises as why the land is only weakly cooled, while the SSTs just westward of it are much lower. Although MSE is transported from sea to land (Fig. 1a) and the region of marine influence extends towards Eastern Europe, homogenization of the cooling pattern between sea and land does not occur. In the following, we investigate the mechanisms that maintain this land–sea contrast in the presence of a strong zonal cross-gradient advection (highlighted by the 2-m mean winds on Fig. 1b), by analyzing the radiative response, the cloud response and associated feedbacks on temperature, and the change in moisture over land and sea.

## 4 Mechanisms leading to a different response over the ocean and above land

### 4.1 Response of the atmospheric radiative and turbulent fluxes

The primary ocean-driven atmospheric response to the THC collapse induces changes in net turbulent fluxes (sensible heat and latent heat fluxes) and in net radiative fluxes (long wave and short wave radiation) which affect the temperature response above land. The net atmospheric surface heat flux anomalies above the ocean are on the order of 85 $W\ m^{-2}$ (Fig. 2a). They are dominated by the reduced latent heat release. Positive values above sea

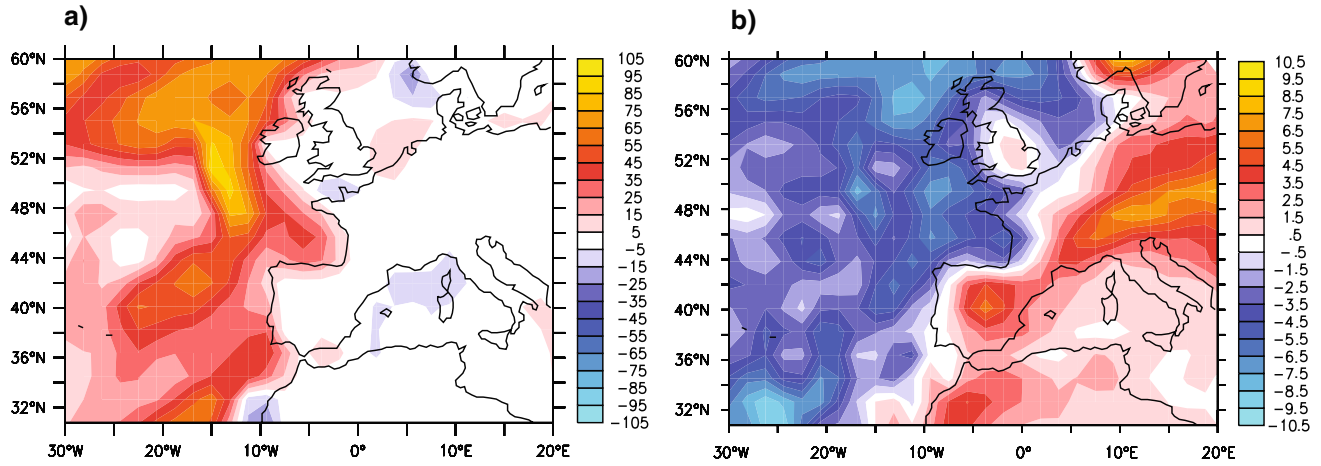


**Fig. 2** **a** Net atmospheric surface heat flux anomalies. **b** Short wave radiation anomalies at the surface. Downward fluxes are positive (W $m^{-2}$). Note that the color scales are different

indicate that the ocean cools the atmosphere and the atmosphere anomalously warms the ocean, to compensate for the reduced ocean heat transport divergence. Thus the ocean is driving the atmospheric cooling. Because the eddy correlation between velocity, pressure and MSE was not diagnosed, we can only determine the change in MSE flux divergence indirectly by assuming it to be the opposite of the change in atmospheric fluxes. The divergence of MSE flux (it is very close to the negative of Fig. 2a), strongly decreases over the ocean. Also over land, the surface MSE flux is 0 (Fig. 2a). The response in TOA flux over land is an increase in downward radiation (Fig. 1c) which implies a reduced convergence of MSE over land. Together, these suggest that there is less transport of MSE from the ocean to the land in response to a THC collapse.

The net flux anomalies at the top of the atmosphere (TOA) are about 10% of the net flux anomalies at the surface (not shown, in agreement with Cheng et al. 2007; their Fig. 4). These TOA fluxes feature enhanced downward fluxes over land (by about 4.5°W $m^{-2}$) suggesting a (secondary) cloud response. The change in short wave radiation at the surface (Fig. 2b) clearly supports the suggestion of a cloud response. We find decreased short wave radiation by about 6.5 W $m^{-2}$ over sea, suggesting an increase of clouds blocking the penetration of short wave radiation; and increased short wave radiation by about 4.5 W $m^{-2}$ over land, suggesting a decrease of clouds allowing more short wave radiation to reach the surface.

## 4.2 Change in clouds and associated feedbacks

### *4.2.1 Cloud radiative forcing and associated changes in radiative fluxes*

Clouds can have multiple effects on the radiation balance. They decrease the incoming short wave radiation at the surface which is a cooling effect, but they also decrease the net outgoing long wave radiation at the surface which is a warming effect. The cloud radiative forcing net effect of clouds in the mid latitudes, however, is to cool the surface which implies that the change in TOA short wave radiation dominates the change in surface long wave radiation (Harrison et al. 1990). Over the ocean, the net reduction mounts to about 60 W $m^{-2}$, over land it becomes about 25 W $m^{-2}$, but only north of the Mediterranean Sea (Fig. 3a). The change in cloud radiative forcing in response to a THC collapse is shown in Fig. 3b. Over the ocean, we find a decrease of the order of 8 W $m^{-2}$ (both in winter and summer, not shown) consistent with an increase of clouds over the ocean. Increased cloud cover over the ocean enhances the cooling of the atmosphere that already results from the anomalous downward (latent heat) flux into the ocean. Above land, an increase of 4 W $m^{-2}$ (mainly in winter, not shown) is consistent with a decrease of cloud cover over land. Decreased cloud cover above land tempers the cooling in the atmosphere which results from the advection of cold air from above sea. We hypothesize that a strong secondary cloud response is set up with a positive feedback over the ocean and a negative feedback above land, enhancing the land–sea contrast in the temperature response. In the following we will explore this hypothesis.

### *4.2.2 Change in liquid water*

The annual mean change in column-integrated liquid water (Fig. 4a) confirms the decrease of liquid water over land by about 0.1 g $m^{-2}$ and the increase of liquid water over sea by about 0.03 g $m^{-2}$, as suggested by the change in short wave radiation (Fig. 2b) and the change in net cooling by clouds as displayed in Fig. 3b. The change in liquid water has a strong seasonality. Liquid water decreases over land mainly

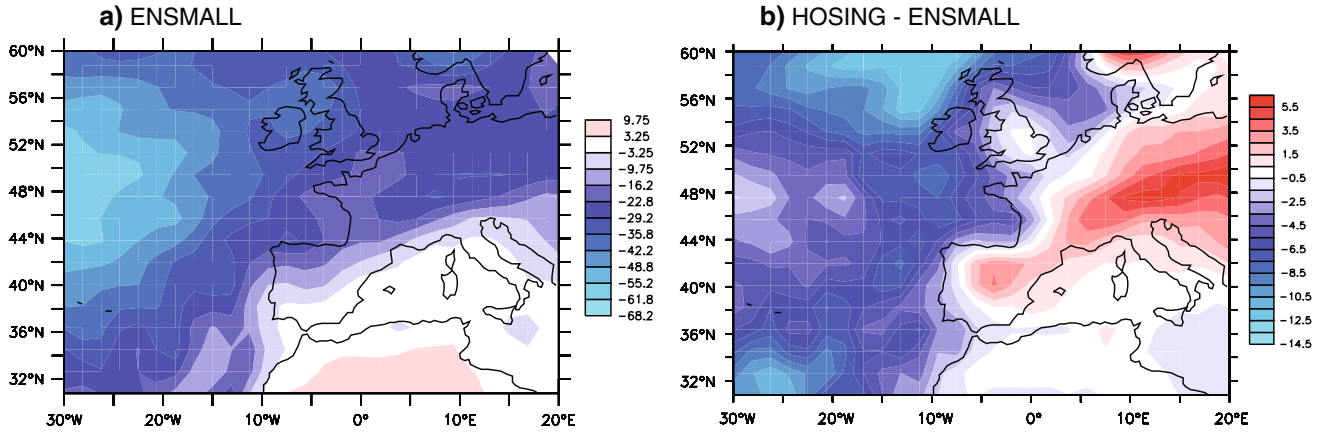


**Fig. 3** Cloud radiative forcing, calculated as the annual mean difference between the radiative fluxes at the top of the atmosphere with clouds and under clear sky conditions (in W $m^{-2}$) in ENSMALL (**a**) and in HOSING–ENSMALL (**b**). Note that the color scales are different

in winter (Fig. 4b) and increases over the ocean mainly in summer (Fig. 4c). So, both seasons contribute to the annual mean pattern. Note that this liquid water response pattern is a column-integrated view of clouds that may have different effects on the radiative fluxes response at different height.

The vertical distribution of the change in liquid water at 48°N shows that the increase over the ocean occurs below 900 hPa both in winter and in summer (Fig. 5). Above land, the decrease of liquid water occurs between 900 and 600 hPa mainly in winter (Fig. 5a).

The cooler air temperature over the ocean in response to the THC collapse (Fig. 1b) results in an increased stability of the atmospheric boundary layer (not shown), reducing entrainment of dryer air at the top of the marine boundary layer. This leads to an increase of lower clouds over the ocean all year long as seen in Fig. 5. Above land, another mechanism must be responsible for the strong decrease of mid level clouds (below 600 hPa) occurring mainly in winter (Fig. 5a). We will explore that now.

#### *4.2.3 Changes in specific humidity and in relative humidity*

The response of cloud cover to a THC collapse is expected to be associated with a similar response in relative humidity, although clouds are a more intermittent phenomenon. Since the 2-m temperature decreases everywhere in response to the THC collapse (Fig. 1b), the specific humidity at the surface is also expected to be lower. First, evaporation decreases, and second, the colder air is more easily saturated. Decreases in temperature and specific humidity have opposing effects on the relative humidity. Figure 6a shows the annual mean response of the specific humidity at the surface. It decreases over the whole domain, by about 2 g $kg^{-1}$ over the ocean and 1.2 g $kg^{-1}$ over land. The response pattern features similar zonal contrasts as the 2-m temperature response. The response in relative humidity shows an increase over sea by about 5% and a decrease over land by about 1% (Fig. 6b). This strong land–sea contrast in the relative humidity response is consistent with the decreased clouds over land and the increased clouds over sea as suggested by Figs. 4 and 5.

In order to understand what causes the land–sea contrast in the relative humidity response, we investigated the respective roles of the temperature and specific humidity changes using the Clausius–Clapeyron equation. A linear decomposition of the change in relative humidity ($\Delta$RH) can be written as a function of the changes in temperature ($\Delta T$) and in specific humidity ($\Delta q$) such that

$$\Delta \mathrm{RH} = \mathrm{RH}\left(\frac{\Delta q}{q} - \frac{0.622 L_v}{RT^2}\Delta T\right)$$

where $R$ is the gas constant for dry air. From a linear decomposition of the change in relative humidity, it can be concluded that the net change in relative humidity is dominated by the negative temperature change over the ocean and by the decrease in specific humidity over land (not shown).

### 4.3 Change in moisture transport: reduced marine influence over Western Europe

Change in moisture transport is the final element that we investigate in order to understand the decrease in cloud cover and relative humidity over land. The change in moisture sink (precipitation minus evaporation, noted P–E) is balanced by the change in moisture divergence by advection. Over the ocean, the annual mean transport of moist air towards land is reduced by about 1 mm $day^{-1}$ (Fig. 7). This reduction is largest in winter (not shown). The reduced transport of moisture towards land is consistent with the strong decrease in evaporation over the ocean related to the strong decrease in latent heat flux (Fig. 2a).

A decomposition of the anomalous advection of moisture $(\Delta(\vec{U}\cdot\vec{\nabla}q))$ into a dynamical term $(\Delta\vec{U}\cdot\vec{\nabla}q)$ and a thermodynamical term $(\vec{U}\cdot\Delta(\vec{\nabla}q))$ indicates that the

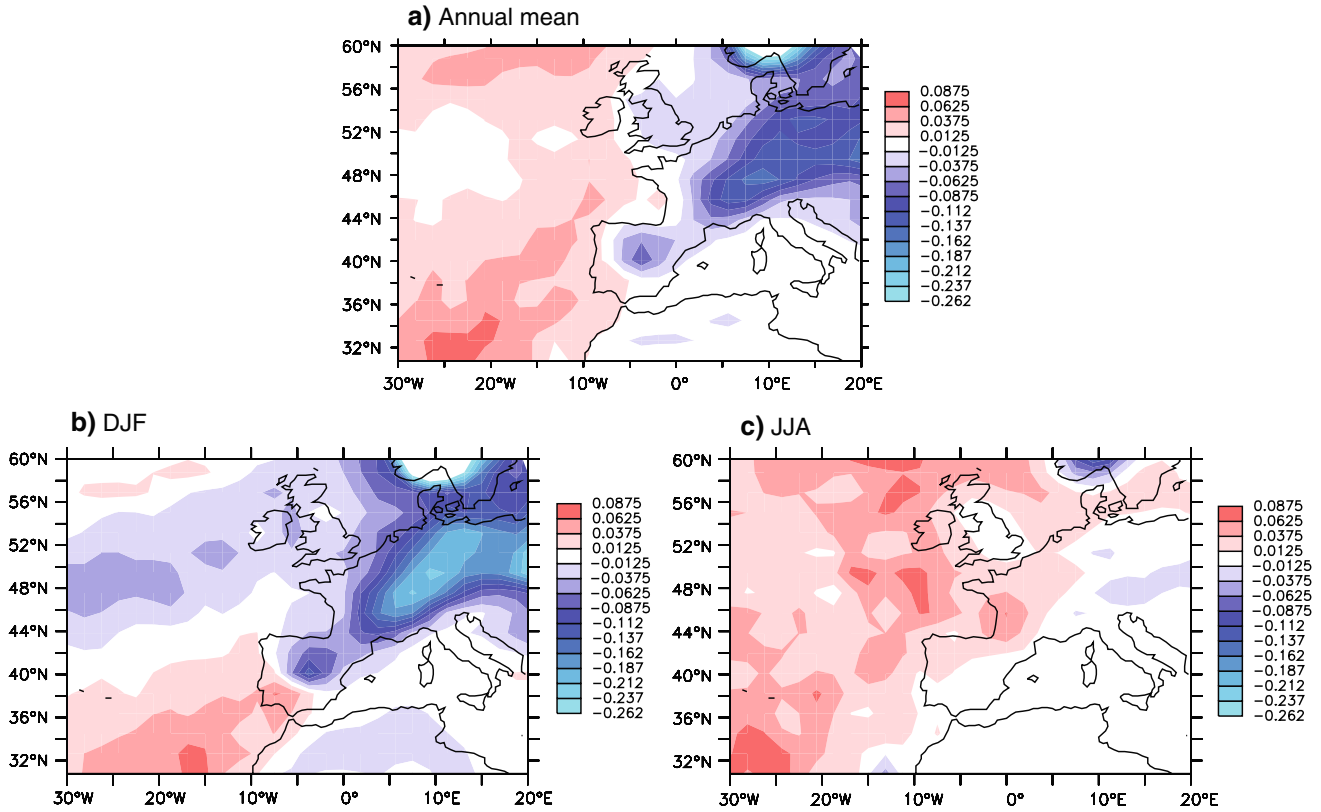


**Fig. 4** Change in column-integrated liquid water (g $m^{-2}$) in annual mean (**a**), in December–January–February (**b**) and in June–July–August (**c**)

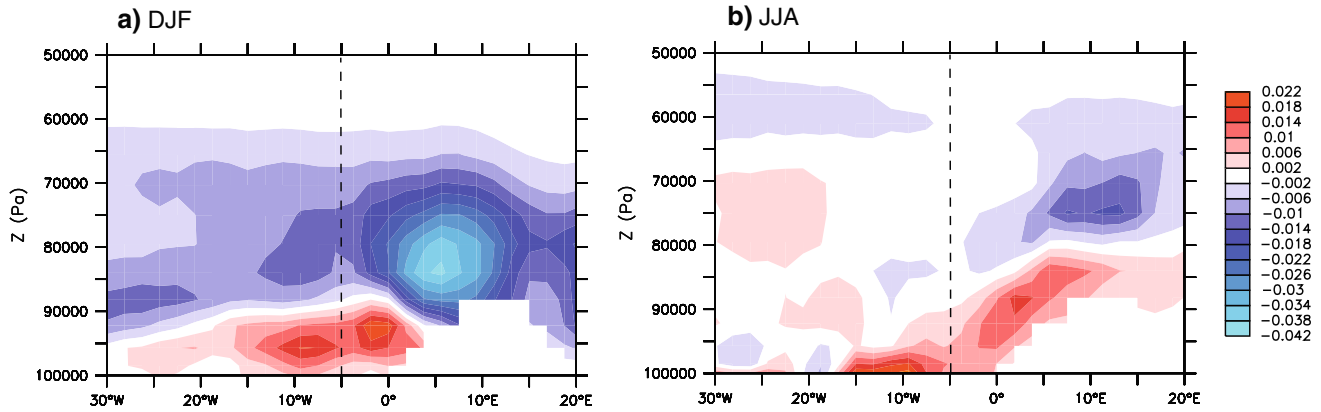


**Fig. 5** Change in liquid water (g $kg^{-1}$) at 48°N in winter (**a**) and in summer (**b**).The *dashed line* indicates the coastline at this latitude

reduction of moisture transport towards land is mainly driven by the decrease in specific humidity (not shown).

As a result, the marine impact on Western European climate is reduced, mainly due to a reduced transport of moisture towards land because of reduced evaporation above the ocean. This results in decreased cloud cover above land, mainly in winter, which acts as a secondary response maintaining the land–sea contrast of the temperature response.

The mechanisms responsible for the strong land–sea contrast in the response of Western European climate to a collapse of the THC are summarized in Fig. 8.

## 5 Comparison between the response over Western Europe and the globally averaged response

Over Western Europe, the vertical profile of the domain-averaged mean temperature shows a cooling of about 2°C from the surface up to 300 hPa. This cooling is dominated by cooling over the ocean (Fig. 9a). In contrast, the vertical profile of the global mean temperature shows a cooling of about 0.6°C up to 300 hPa which is dominated by cooling over land (Fig. 9b). This global cooling is consistent with the response described in Joshi08 for

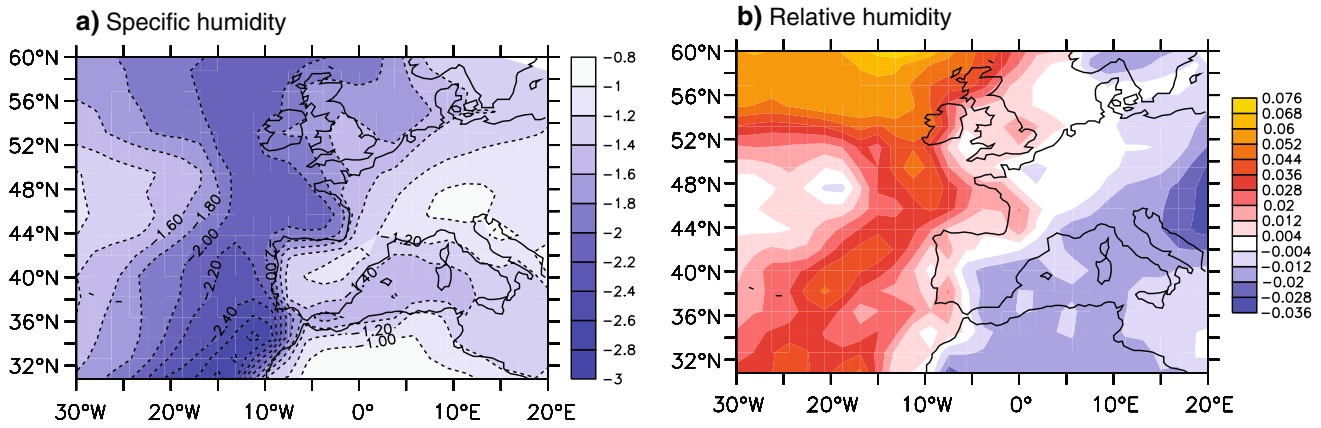


**Fig. 6** Annual mean changes in surface specific humidity (**a**, g kg$^{-1}$) and in relative humidity (**b**, fraction)

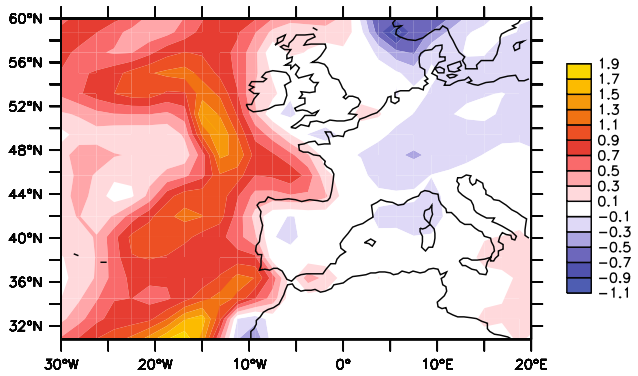


**Fig. 7** Annual mean change in P–E (mm day$^{-1}$)

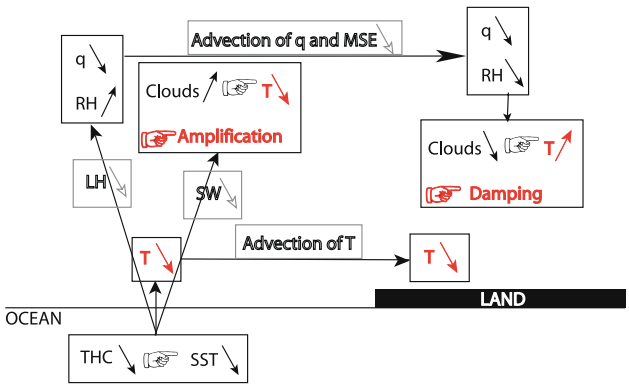


**Fig. 8** Schematic of the mechanisms responsible for the land–sea contrasts discussed in the paper

instance, but it is opposite to the land–sea contrast over Western Europe.

Joshi08 suggest that changes in the environmental lapse rate ($\Gamma = -\partial T/\partial z$) can explain the land–sea contrast. In their study, $\Gamma$ increases in response to a homogeneous global SST cooling. This implies that the cooling in the upper troposphere is stronger than at the surface. The environmental lapse rate increases even more over sea, and therefore, near the surface, the cooling over sea is smaller than over land. This result found by Joshi08 is confirmed in our study on the global scale: near the surface the cooling over sea is smaller than over land, but the lapse rate response in our study is opposite to the one found by Joshi08, the lapse rate decreases in response to cooling and the cooling in the upper troposphere is everywhere smaller than at the surface (Fig. 9b). However in Western Europe and in the North-eastern Atlantic, and in particular above the cold SST anomaly near Western Europe, the environmental lapse rate decreases more over sea than over land in response to the cooling due to the THC collapse (Fig. 10). The decrease in $\Gamma$ is strongest over the North-eastern Atlantic, where the SST anomalies are the largest. Higher up in the atmosphere, land–sea contrasts and regional differences become smaller. To be compatible with the strong SST forcing and the decrease in $\Gamma$, the anomaly in the upper troposphere must therefore be smaller than at the surface. Away from the North-eastern Atlantic and Western Europe, the non homogeneous surface forcing is weaker and the cooling in the upper troposphere is larger than (or even opposite to) the surface cooling, as in Joshi08.

The change in environmental lapse rate can be decomposed into a term containing temperature effects that are due to changes in saturated lapse rate, and a term containing moisture effects that are due to changes in relative humidity such that

$$\Delta\Gamma = \Delta\Gamma_S + \Delta\Gamma_M$$

where $\Delta\Gamma_S$ is the saturated lapse rate (e.g. Stone and Carlson 1979) and the moist lapse rate $\Delta\Gamma_M$ is approximated by $\Delta\Gamma - \Delta\Gamma_S$. In reality, the temperature effect in the change in environmental lapse rate is smaller than $\Delta\Gamma_S$, because the air is not saturated, and the estimate of the temperature effect is only an upper bound. Because we want to demonstrate that the temperature effect is not the

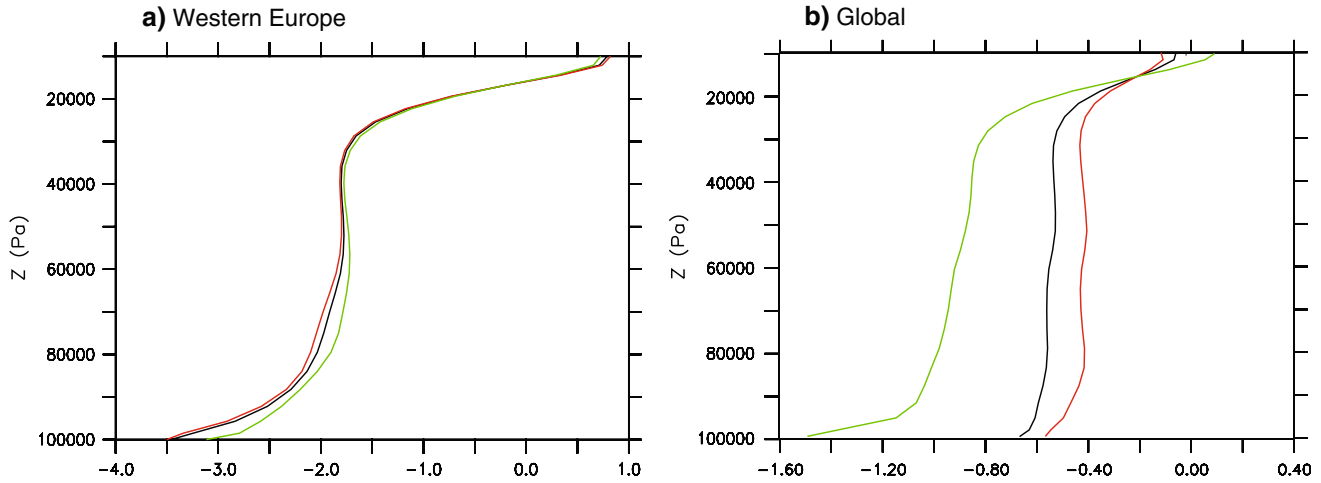


**Fig. 9** Temperature change (in °C) computed as the difference between HOSING and ENSMALL over Western Europe (**a**) and over the globe (**b**). The response is averaged over the whole region (*black*), over the ocean (*red*) and over land (*green*). Note the different horizontal axis

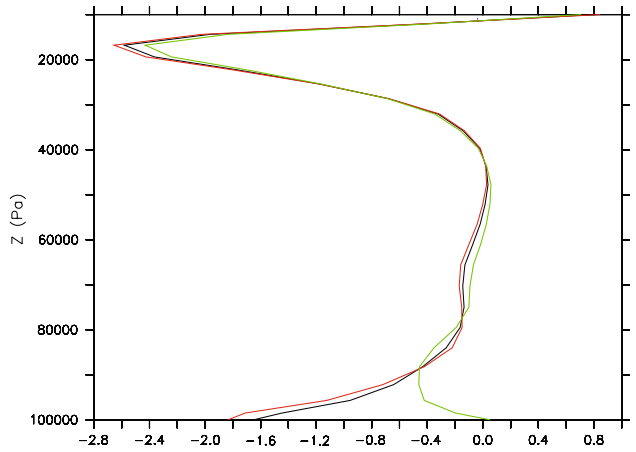


**Fig. 10** Change in environmental lapse rate computed as the difference between HOSING and ENSMALL in Western Europe, averaged over the whole region (*black*), over the ocean (*red*) and over land (*green*) (°C $km^{-1}$)

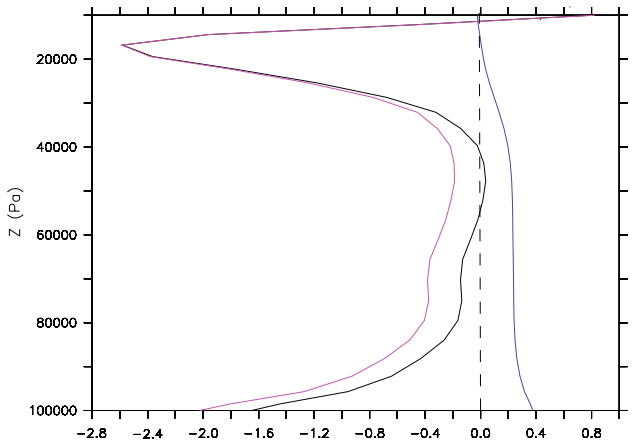


**Fig. 11** Change in lapse rate averaged over Western Europe (*black*, °C $km^{-1}$). Changes in temperature effects (*blue*) and in moisture effects (*magenta*) are also shown

main process causing the change in environmental lapse rate here, this difference is irrelevant.

In our study, the global mean change in environmental lapse rate can be explained by the temperature effect. However, above the cold SST anomaly near Western Europe, the change in environmental lapse rate is dominated by the moisture effect (i.e. the change in relative humidity) over the whole column (Fig. 11) and in particular over the ocean as a result of the non homogeneous SST forcing. Moreover over Western Europe, the change in saturated lapse rate ($\Delta\Gamma_S$) is of opposite sign compared to the change in environmental lapse rate ($\Delta\Gamma$). Therefore, temperature effects cannot be the cause of the decrease of $\Gamma$ and changes in moisture have to be the main cause. These moisture changes consist of an increase of the relative humidity and an associated increase of clouds over the SST minimum (Figs. 4 and 6b).

## 6 Summary and conclusions

The response of Western European climate to a collapse of the THC has been investigated in the ECHAM5/MPI-OM coupled model under global change conditions. The primary response is ocean-driven. This response features a strong zonal gradient of surface air temperature between the ocean and the continent. Advection of temperature and moist static energy from the ocean to the continent is expected to homogenize this gradient. This homogenization, however, does not take place. We investigated the causes which maintain the ocean–land gradient. Above the ocean, more low clouds are formed due to an increase in relative humidity and a more stable marine boundary layer. These clouds have a cooling effect over the ocean which enhances the cooling due to the primary ocean-driven response. A decrease in convergence of moist static energy

above land is responsible for a decrease of clouds above land. The effect of this is to warm the atmosphere over land, thereby weakening the cooling over land that results from advection of colder and dryer air from the sea. The secondary cloud response therefore acts to enhance the land–sea contrast in surface air temperature response.

It appears that the surface temperature forcing pattern is a crucial element to understand the atmospheric response. On the global scale, we find a land–sea contrast with cooling above land being larger than cooling over the ocean. However, in Western Europe and especially over the cold SST anomalies west of the continent, we find an opposite land–sea contrast. The difference arises from the non homogeneous SST forcing. Above the cold SST anomalies, the change in lapse rate is more affected by a change in moisture, while over the whole globe, it is more affected by a change in temperature.

**Acknowledgments** The ESSENCE project, lead by Wilco Hazeleger (KNMI) and Henk Dijkstra (UU/IMAU), was carried out with support of DEISA, HLRS, SARA and NCF (through NCF projects NRG-2006.06, CAVE-60–023 and SG-06-267). We thank the DEISA Consortium (co-funded by the EU, FP6 projects 508830/031513) for support within the DEISA Extreme Computing Initiative (www.deisa.org). The authors thank Andreas Sterl (KNMI), Camiel Severijns (KNMI), and HLRS and SARA staff for technical support. We thank two anonymous reviewers for their comments that have helped to improve the manuscript.

## References

Bryden HL, Longworth HR, Cunningham SA (2005) Slowing of the Atlantic meridional overturning circulation at 25°N. Nature 438(7068):655–657. doi:10.1038/nature04385

Chang P, Zhang R, Hazeleger W, Wen C, Wan X, Ji L, Haarsma RJ, Breugem W–P, Seidel H (2008) Oceanic link between abrupt changes in the North Atlantic Ocean and the African monsoon. Nature Geoscience. doi:10.1038/ngeo218

Cheng W, Bitz CM, Chiang JCH (2007) Adjustment of the Global Climate to an Abrupt Slowdown of the Atlantic Meridional Overturning Circulation. Geophys Monogr 1973:295–314

Cunningham SA, Kanzow T, Rayner D, Baringer MO, Johns WE, Marotzke J, Longworth HR, Grant EM, Hirshi JJ, Beal LM, Meinen CS, Bryden HL (2007) Temporal variability of the Atlantic meridional overturning circulation at 26.5°N. Science 317(5840):935–938. doi:10.1126/science.1141304

Dong B-W, Sutton RT (2002) Adjustment of the coupled ocean-atmosphere system to a sudden change in the Thermohaline Circulation. Geophys Res Lett. doi:10.1029/2002GL015229

Harrison EF, Minnis P, Barkstrom BR, Ramanathan V, Cess RD, Gibson GG (1990) Seasonal variation of cloud radiative forcing derived from the earth radiation budget experiment. J Geophys Res 95:18687–18703. doi:10.1029/JD095iD11p18687

Joshi MM, Gregory JM, Webb MJ, Sexton DMH, Johns TC (2008) Mechanisms for the land-sea warming contrast exhibited by simulations of climate change. Clim Dyn. doi:10.1007/s00382-007-0306-1

Manabe S, Stouffer RJ (1988) Two stable equilibria of a coupled ocean–atmosphere model. J Clim 1:841–866. doi:10.1175/1520-0442(1988)001<;0841:TSEOAC>;2.0.CO;2

Manabe S, Stouffer RJ (1999) The role of thermohaline circulation in climate. Tellus 51 A-B:91–109

Marsland SJ, Haak H, Jungclaus JH, Latif M, Röske F (2003) The Max-Planck-Institute global ocean/sea ice model with orthogonal curvilinear coordinates. Ocean Model 5:91–127. doi:10.1016/S1463-5003(02)00015-X

Nakicenovic N, et al. (2000) Special Report on Emissions Scenarios: A special report of working group III of the Intergouvernmental panel on climate change. Cambridge University Press, Cambridge, UK. Available online at www.grida.no/climate/ipcc/emission/index.htm

Roeckner E, Bäuml G, Bonaventura L, Brokopf R, Esch M, Giorgetta M, Hagemann S, Kirchner I, Kornblueh L, Manzini E, Rhodin A, Schlese U, Schulzweida U, Tompkins A (2003) The atmospheric general circulation model ECHAM 5. Part I: model description. Tech. Rep. 349. Max-Planck-Institut für Meteorologie, Hamburg

Schmittner A, Latif M, Schneider B (2005) Model projections of the North Atlantic thermohaline circulation for the 21st century assessed by observations. Geophys Res Lett. doi:10.1029/2005GL024368

Sterl A, Severijns C, Dijkstra H, Hazeleger W, van Oldenborgh GJ, van den Broeke M, Burgers G, van den Hurk B, van Leeuwen PJ, van Velthoven P (2008) When can we expect extremely high surface temperature? Geophys Res Lett. doi:10.1029/2008GL034071

Stone PH, Carlson JH (1979) Atmospheric lapse rate regimes and their parameterization. J Atmos Sci 36(3):415–423

Stouffer RJ, Yin J, Gregory JM, Dixon KW, Spelman MJ, Hurlin W, Weaver AJ, Eby M, Flato GM, Hasumi H, Hu A, Jungclaus JH, Kamenkovich IV, Levermann A, Montoya M, Murakami S, Nawrath S, Oka A, Peltier WR, Robitaille DY, Sokolov A, Vettoretti G, Weber SL (2006) Investigating the causes of the response of the thermohaline circulation to past and future climate changes. J Clim 1365–1387. doi:10.1175/JCLI3689.1

Sutton RT, Dong B, Gregory JM (2007) Land/sea warming ratio in response to climate change: IPCC AR4 model results and comparison with observations. Geophys Res Lett. doi:10.1029/2006GL028164

Vellinga M, Wood RA (2002) Global climatic impacts of a collapse of the Atlantic thermohaline circulation. Clim Change 251–267. doi:10.1023/A:1016168827653

Vellinga M, Wood RA (2006) Impacts of thermohaline circulation shutdown in the twenty-first century. Clim Change. doi: 10.1007/s10584-006-9146-y

Yin J, Stouffer RJ (2007) Comparison of the stability of the Atlantic thermohaline circulation in two coupled atmosphere–ocean general circulation models. J Clim 20(17):4293–4315